ORIGINAL ARTICLE

Ultrasound Biomicroscopy of the Aging Rhesus Monkey Ciliary Region

ADRIAN GLASSER, PhD, MARY ANN CROFT, MS, LYNDIA BRUMBACK, MS, and PAUL L. KAUFMAN, MD

College of Optometry, University of Houston, Houston, Texas (AG), Department of Ophthalmology and Visual Sciences (AG, MAC, PLK) and Department of Biostatistics and Medical Informatics (LB), University of Wisconsin-Madison, Madison, Wisconsin

ABSTRACT: Ultrasound biomicroscopy of the living rhesus monkey ocular ciliary region was undertaken to identify age-dependent changes that might relate to the progression of presbyopia. Monkeys were anesthetized and pharma-cologically cyclopleged, the eyelids were held open with a lid speculum, and sutures were placed beneath the medial and lateral rectus muscles. Ultrasound biomicroscopy imaging of the nasal and temporal quadrants of the eye were performed, and the live images were recorded to videotape. Subsequent image analysis was performed to obtain objective morphometric measurements of the ciliary body region. The ciliary body inner radius of curvature, outer radius of curvature, inner arc length, area, thickness, perimeter, zonular fiber length, and circumlental space were measured. Zonular space was calculated. The circumlental space decreased with increasing age in the temporal quadrant. The other morphologic measurements were not significantly correlated with age or body weight. Most morphologic measurements were significantly different comparing temporal vs. nasal quadrants. Bifurcation of the posterior zonular fibers was frequently observed. Although temporal circumlental space was the only measurement found to change with age, ultrasound biomicroscopy of the living rhesus ciliary region did identify distinct nasal vs. temporal asymmetries, which may reflect anatomical requirements for convergence-associated accommodation. (Optom Vis Sci 2001;78:417–424)

Key Words: aging, zonular fibers, ciliary body, ultrasound biomicroscopy, accommodation, presbyopia, rhesus monkeys

ge changes in human ciliary muscle morphometry have been identified from histologic sections. With increasing age between 33 and 87 years, the muscle area decreases, length decreases, width remains constant, distance between the scleral spur and inner apex of the muscle decreases, areas of the longitudinal and the reticular portions decrease, and area of the circular portion increases. In addition, the configuration of the unaccommodated ciliary muscle of older human eyes is more like that of a young accommodated ciliary muscle. Such configurational changes occur with the same relative age course as the loss of accommodation and have been implicated as a possible factor in presbyopia in humans. Histologic study of the atropinized rhesus monkey ciliary muscle shows that it becomes shorter and reduced in width, overall area, and area of the longitudinal portion with increasing age. 1, 2

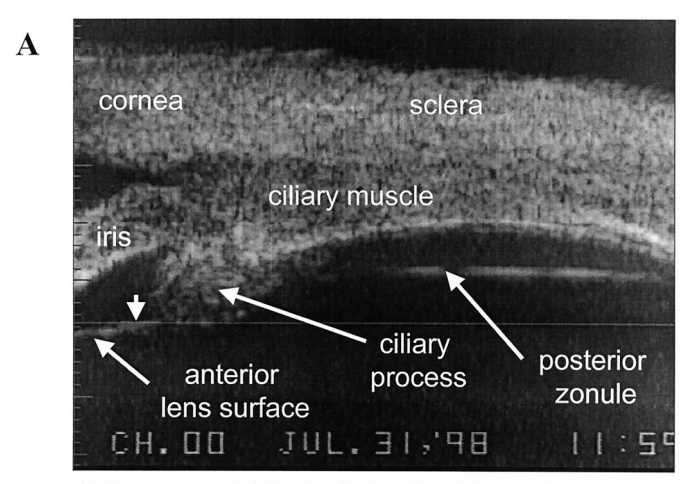
Rhesus monkeys develop presbyopia with the same relative age course as humans.³ Age-related structural neuromuscular changes with a similar age course as the loss of accommodation are report-

ed,⁴ although their relevance to ciliary muscle contractility is not clear. Contractile responses of isolated rhesus ciliary muscle strips *in vitro* do not decrease with age,⁵ and there are no alterations in the number and affinity of muscarinic receptors (as measured by ³H-QNB binding) or in Km and Vmax for choline acetyltransferase and acetylcholinesterase, the biosynthetic and biodegradative enzymes for the cholinergic neurotransmitter acetylcholine.⁶ Although age changes in the ciliary muscle of humans and monkeys differ,¹ both show decreases in length, area of the longitudinal portion, and total area of the ciliary muscle with age.^{1, 2}

Although age changes in the crystalline lens may fully account for the age-related loss of accommodation in humans,^{7, 8} a loss of elasticity of the posterior attachments of the ciliary muscle and of the choroid may play a major role in the development of presbyopia in rhesus monkeys.^{1, 2, 9} Thus, we cannot exclude the possibility that extralenticular changes also occur in the human eye with increasing age that may contribute to presbyopia. Reciprocal studies to determine whether lenticular sclerosis occurs in monkeys and

choroidal elasticity is lost in humans have yet to be done. The present ultrasound biomicroscopic (UBM) study was undertaken in an attempt to obtain quantitative morphometric data on the ciliary region of *living* rhesus monkeys encompassing the age over which accommodative decline is most pronounced.

UBM relies on the tissue structures being examined scattering ultrasound waves that are subsequently detected by the ultrasound transducer. 10 The lateral and axial resolutions of a 50-MHz transducer are ~50 µm and 37 µm, respectively. 10 Although lacking the resolution and the ability of histologic methods to distinguish between tissue types (such as muscle and connective tissue), UBM allows direct, real-time imaging of the ciliary region of the living, intact eye, including structures not otherwise visible, and provides a digital image from which morphometric measurements can readily be made. Numerous prior studies have undertaken quantitative morphometric measurements using UBM including similar parameters to those measured here as well as considerably more detailed measurements. 11-15 The plane of the image section can be identified and selected with minimal manipulation of the eye and transducer (Fig. 1). Magnetic resonance imaging (MRI) has been used to measure changes in the human eye with accommodation and aging. 16, 17 Although MRI provides images of the entire globe



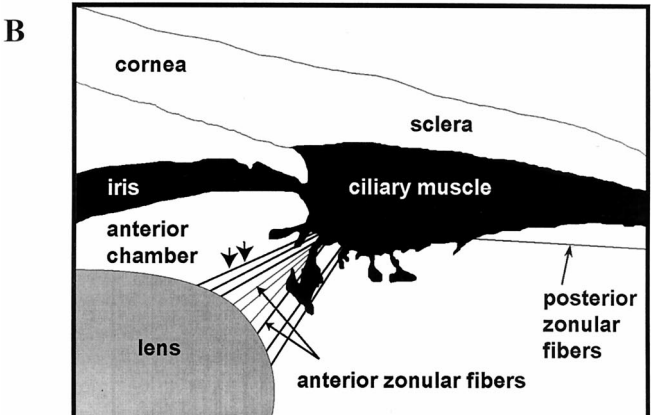


FIGURE 1.

Ultrasound biomicroscopy provides a tool to image the ciliary region of the living monkey eye (A) and visualize the major components of the accommodative apparatus shown schematically (B). Arrowheads identify the anterior leaf of the anterior zonule that can be seen with UBM. B: the finer anterior zonular fibers are shown diagrammatically with thinner lines.

from which measurements such as lens equatorial diameter can be made, the low temporal and spatial resolution prohibit fine orientation of the eye and morphometric measurement of the ciliary body such as can be done using the relatively higher resolution, real-time UBM images. We report here an *in vivo* UBM study of the ciliary region of atropinized rhesus monkey eyes. A summary of this work has been published previously.¹⁸

METHODS

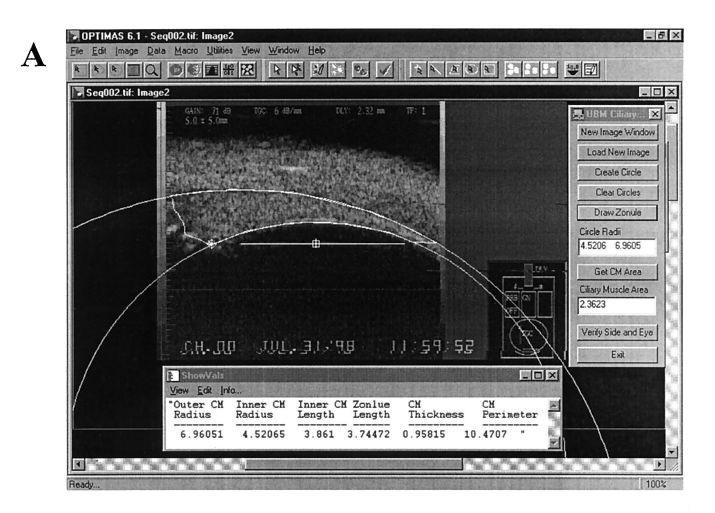
Animals and Procedures

Thirteen rhesus monkeys, aged 3 to 23 years were used (seven males and six females) weighing 4.4 to 13.7 kg. All studies were in accordance with institutionally approved animal protocols and with the Association for Research in Vision and Ophthalmology Statement for the Use of Animals in Ophthalmic and Vision Research. Five of the monkeys had previously undergone bilateral, complete 360° iridectomies for other experimental protocols. Monkeys were anesthetized with intramuscular ketamine (10 mg/ kg) and acepromazine (0.1 mg/kg). The right eye of each monkey was cyclopleged by instilling two drops of 5% homatropine topically. The monkey was placed supine with the head immobilized in a head holder. 4-0 Silk sutures were placed beneath the medial and lateral rectus muscles. A Plexiglas scleral cup was inserted beneath the eyelids of the right eye and filled with sterile saline or Goniosol (Bausch & Lomb, Tampa, FL).¹⁰ In one or two cases in the younger animals when the scleral cup was too large to fit under the eyelids, the lids were held open with a lid speculum, and K-Y Jelly (Johnson & Johnson, New Brunswick, NJ) with a higher viscosity than Goniosol was applied to the eye. The eye was adducted by applying traction to the lateral rectus muscle suture, and imaging was performed on the temporal ciliary region using a UBM (Humphrey Instruments, Model-840, 50 MHz, 50 µm lateral resolution, and 37 µm axial). The eye was then abducted with traction on the medial rectus muscle suture, and imaging was performed on the nasal ciliary region. Because the UBM transducer could be used at an angle, it was not necessary to rotate the eye excessively to achieve this imaging. To image the posterior zonular fibers most clearly, the eye and transducer were carefully positioned to ensure that the posterior zonular fibers were oriented horizontally in the image. The live video image was recorded onto videotape using a Sony S-VHS VCR. Image analysis was subsequently performed on the videotaped images using a PC-based image analysis system (Optimas Image analysis software [Media Cybernetics, Silver Spring, MD] and an IC-PCI frame grabber board [Imaging Technology Incorporated, Bedford, MA]) (Fig. 2A).

Image Analysis

From the videotape recordings, five to seven static images of the nasal and temporal quadrants of the eye were acquired and stored to disk. An objective geometric analysis was performed on three images of each of the nasal and temporal quadrants. Only images in which all the necessary landmarks were visible were selected for analysis (Fig. 2). An attempt was made to objectively identify the ciliary region that included the ciliary muscle but excluded obviously protruding ciliary processes. Three points were identified

along the inner curvature of the ciliary body, and another three points were identified along the inner curvature of the sclera adjacent to the ciliary muscle. A circle was described through each set of three points (Fig. 2A). The center and radius of curvature of each circle was computed by calculating the intersection point of the two perpendicular bisectors of the three points. The inner and outer circle defined the inner and outer ciliary body surfaces, respectively. A horizontal line segment was drawn along the posterior zonular fiber to intersect the inner circle at two locations: (1) posteriorly at the posterior origin of the zonular fibers on the ciliary body and (2) anteriorly at the anterior insertion of the zonular fibers at the ciliary processes (the inner apical point). The outline of the ciliary body was then traced by hand with a mouse cursor from the scleral spur. The scleral spur was identified as the point where the tracing of the outer circle departs from the sclera. Although the departure point is not always obvious on each image, it is seen in more anteriorly located images that do not include the posterior landmarks (Fig. 3A). This is an anatomically distinct junction



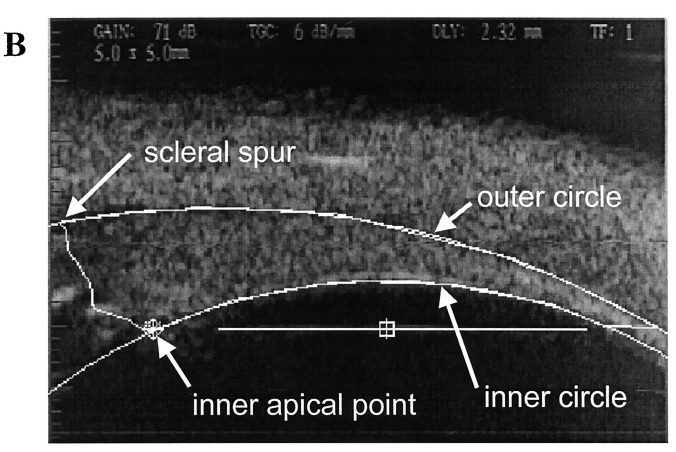
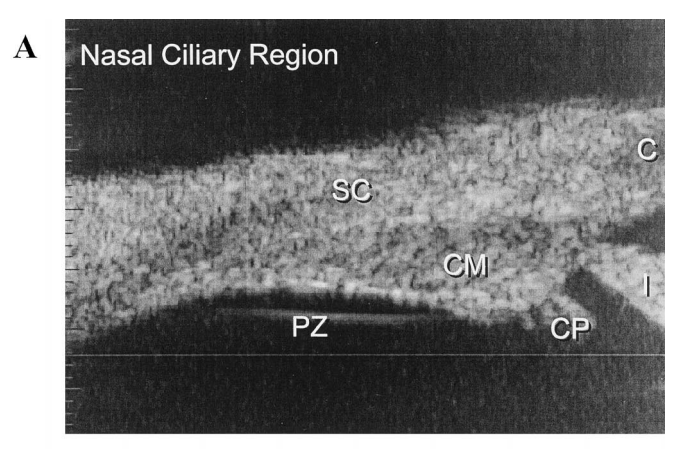


FIGURE 2.

The Optimas image analysis program was used to do an objective morphometric analysis of the ciliary region. A: two circles were described through three points each on the inner and outer surfaces of the ciliary body region. B: a horizontal line was drawn along the clearest portion of the posterior zonular fibers, and starting from the scleral spur (obscured by the overlay), the outline of the ciliary body region was traced. The macro automatically calculated and marked the line segment along the zonular fibers and the intersection points of the inner circle, obviating the need to draw the horizontal line to meet the circle.

between the sclera and the anterior ciliary body. The continuous outline was drawn from the scleral spur on the outer circle, across the anterior face of the ciliary body to the inner apical point, along the chord of the inner circle (along the inner surface of the ciliary body), to the point of the posterior insertion of the zonular fibers at the inner circle, across the posterior ciliary body horizontally to the outer circle, and along the chord of the outer circle of the sclera back to the corneo-scleral spur. Although the anterior face of the ciliary body is poorly defined, this line was traced midway between the discontinuous structures on one side representing the ciliary processes and the continuous structure on the other side representing the ciliary body proper (see Fig. 3A, for example). The inner radius of curvature, outer radius of curvature, inner arc length (the distance along the perimeter of the inner circle between the anterior and posterior intersection points of the line describing the posterior zonular fibers), area, ciliary region thickness (the distance between the outer and inner circles along the line joining the inner apical point and the center of the inner circle), perimeter, zonular fiber length (inner apical point to posterior intersection of posterior zonule with inner circle), zonular space (geometrically calculated by taking the maximum distance from the posterior zonule to the inner circle describing the inner aspect of the ciliary body), and circumlental space were each measured. The circumlental space was measured from the inner apical point to the point of insertion



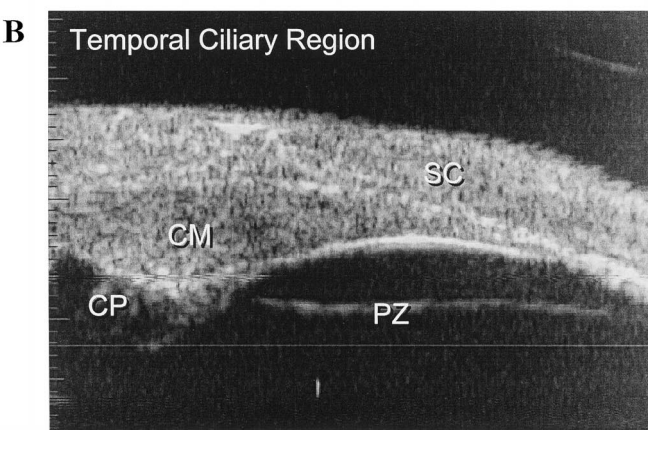


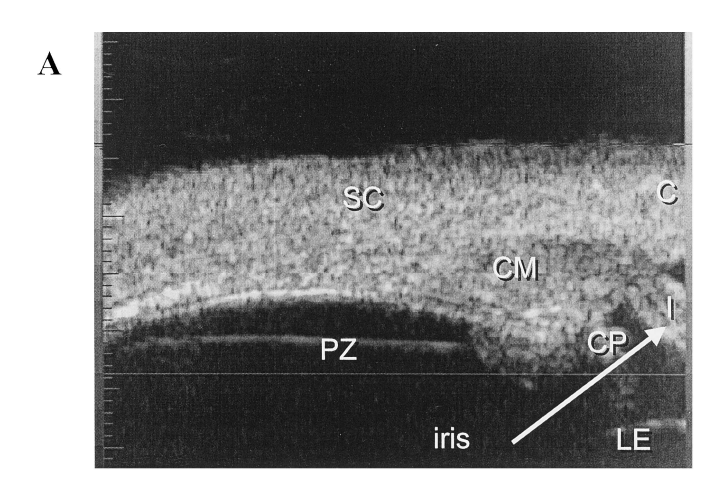
FIGURE 3.

Typical images of the (A) nasal and (B) temporal quadrants of the rhesus monkey ciliary region. Distinct nasal/temporal asymmetries are evident directly from the images and were confirmed by quantitative image analysis (see text). C, cornea; CM, ciliary muscle; CP, ciliary process; I, iris; PZ, posterior zonule; SC, sclera.

of the anterior zonular fibers at the lens equator (Fig. 4 A and B). In some instances, this distance could only be measured in images other than that on which all other measures were made. Although this distance does not necessarily represent the true circumlental space (i.e., the shortest distance between ciliary body and lens equator) because the orientation of the eye and UBM transducer were rigorously controlled, the same anatomical distance was measured from one eye to the next.

Data Analysis

For each animal, the mean and standard deviation of three of each morphologic measurements (outer ciliary body [CB] radius, inner CB radius, inner CB length, zonule length, zonule space, CB thickness, CB perimeter, ciliary muscle [CM] area, and circumlental space [each in the temporal and nasal quadrants]) were computed. Exploratory data analyses included linear regression and paired t-tests. The morphologic measurements were each regressed on age and weight to determine whether any linear relationships existed. Paired t-tests were used to determine whether the morphologic measurements were significantly different in the nasal vs. temporal quadrants.



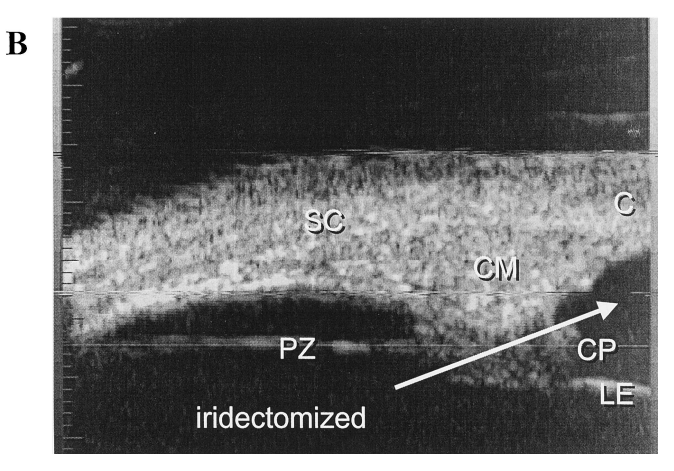


FIGURE 4.

Comparison of the nasal ciliary body regions of a (A) normal and (B) iridectomized eye of two different rhesus monkeys. Besides the obvious absence of the iris, no other pathology is evident. A: left eye, 10 years old, 13.86 kg, male. B: left eye, 22 years old, 5.85 kg, female. C, cornea; CM, ciliary muscle; CP, ciliary process; I, iris; PZ, posterior zonule; SC, sclera; LE, lens equator.

RESULTS

The UBM images clearly show the presence or the absence of the iris in the normal and iridectomized eyes (Fig. 4). With the posterior zonular fibers oriented horizontally in the UBM image, maximal ultrasound scatter results and fine detail of the zonular fibers can be seen. Besides the youngest male with a body weight similar to that of the females, the body weights of the males were heavier than that of the females.

The only morphologic measurement significantly (at the α = 0.05 level) correlated with age was temporal circumlental space (Fig. 5A). Temporal circumlental space decreased with age (N = 12, slope = -0.01, SE = 0.0044, p = 0.041). Nasal outer CB radius and temporal inner CB radius were marginally correlated with age. Nasal outer CB radius increased with age (N = 13, slope)= 0.14, SE = 0.065, p = 0.055) (Fig. 5F) and temporal inner CB radius decreased with age (N = 13, slope = -0.03, SE = 0.018, p = 0.093) (Fig. 5G). None of the morphologic measurements were significantly (at the $\alpha = 0.05$ level) correlated with weight (data not shown). Most morphologic measurements were significantly different comparing temporal vs. nasal quadrants (Table 1). Outer and inner CB radii were smaller in the temporal quadrant, whereas inner CB length, zonule length, zonule space, CB perimeter, and CM area were larger (Table 1 and Fig. 3). No nasal-temporal difference in ciliary body thickness was seen. The posterior zonular fibers in the nasal quadrant appeared closer to the base of the ciliary body and were substantially shorter than in the temporal quadrant.

Qualitative examination of the tracing pattern of the ciliary muscle perimeter in young and old monkeys did not reveal any trend that could be attributed to age (Fig. 6).

In accordance with previous scanning electron microscopic (SEM) descriptions of the posterior zonular fibers of rhesus monkey eyes, 19, 20 the live videographically recorded UBM images also showed that bundles of zonular fibers extend from the posterior insertion of the ciliary muscle to the apices of the ciliary processes and appear to insert in the valleys between the ciliary processes. Such examples were most clearly observed in the temporal quadrants of many of the eyes examined. Images from the nasal quadrant showed this less frequently and less clearly. The live videography as well as the grabbed images (Fig. 7) showed many examples of an apparent bifurcation of the posterior zonular fiber bundles as they coursed from the posterior attachment of the ciliary muscle toward the ciliary body. The outer bundles appeared to pass into the valleys between the ciliary processes apparently to terminate on the lateral walls or near the tips of the processes. After branching, the inner bundles passed between the tips of the processes and appeared to continue toward the lens anterior or posterior equatorial surfaces. Due to an inability to image the nasal zonular fibers as clearly as the temporal fibers, zonular bifurcation was observed less frequently and less distinctly in the nasal quadrant of the eye. The area underlying and spanned by the posterior zonular fibers in the temporal quadrant of the eye was substantially larger than that observed in fixed tissues processed for SEM.²⁰ In the nasal quadrant, the area underlying and spanned by the posterior zonular fibers was considerably reduced with respect to that in the temporal quadrant.

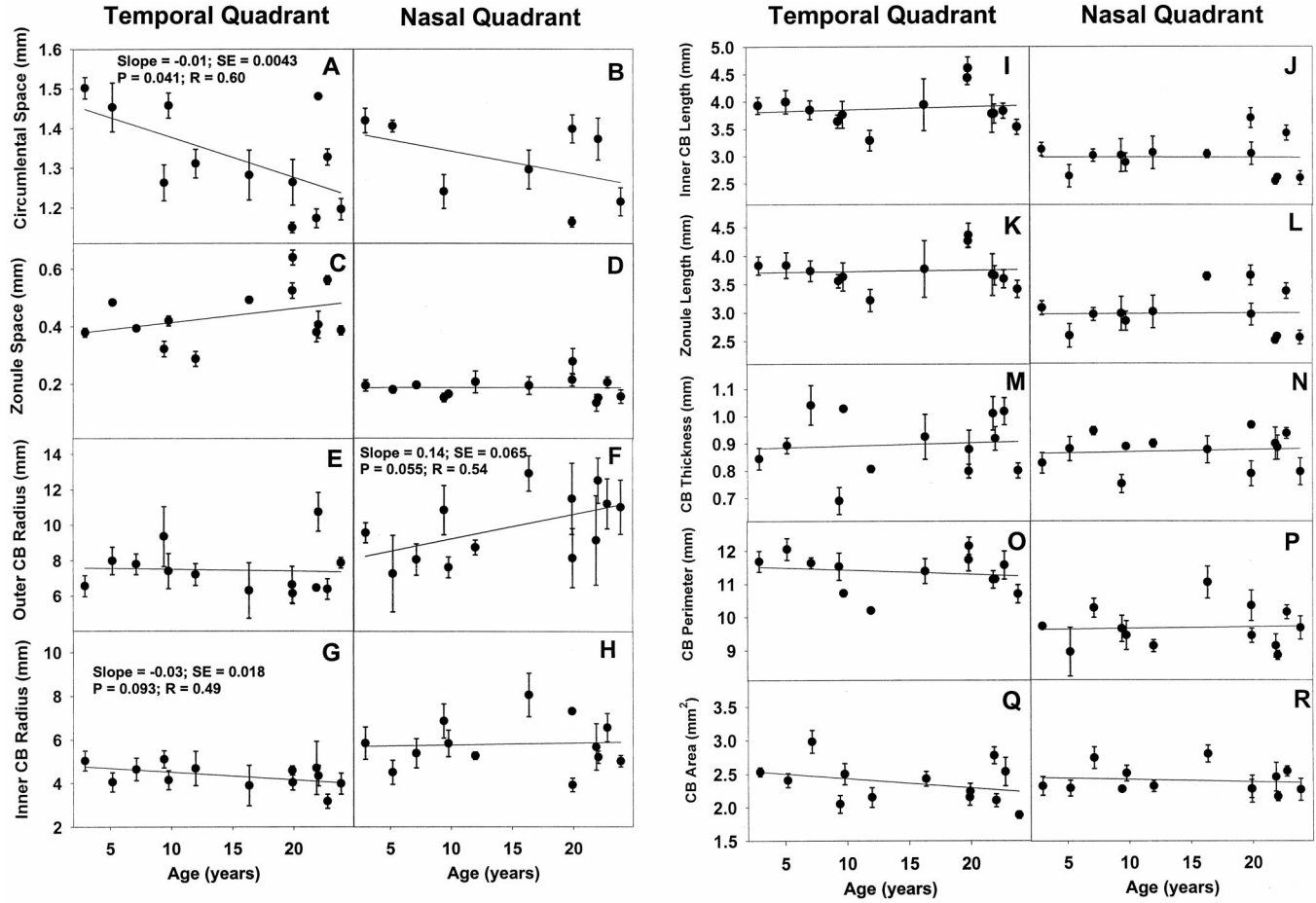


FIGURE 5.

Mean \pm SD of three measurements from each animal for each morphologic measurement. Solid line in each panel indicates fit from linear regression. A: circumlental space in the temporal quadrant of 12 of the 13 rhesus monkeys (circumlental space could not be measured in one monkey) shows a significant decrease with increasing age.

TABLE 1. Comparison of morphologic measurements in temporal and nasal quadrants

Measurement ^a	$\begin{array}{c} {\sf Difference} \\ ({\sf Temporal} - {\sf Nasal})^b \end{array}$	SEM	p Value ^c
Circumlental space (mm)	0.01	0.03	0.7
Zonule space (mm)	0.25	0.02	< 0.0001
Outer \overrightarrow{CB} radius $(mm)^d$	-2.44	0.58	0.0012
Inner CB radius (mm)	-1.90	0.38	0.0003
Inner CB length (mm)	0.90	0.10	< 0.0001
Zonule length (mm)	0.74	0.11	< 0.0001
CB thickness (mm)	0.03	0.02	0.23
CB perimeter (mm)	1.67	0.21	< 0.0001
CM area (mm ²)	0.27	0.06	0.0008

^a For all measures, N = 13 except circumlental space, where N = 8 (circumlental space was only measured on eight monkeys in the nasal quadrant).

DISCUSSION

We have measured monkeys up to age 25 years. Rhesus monkeys live to about 30 to 35 years in captivity, and accommodation is completely lost after 30 years of age.³ Thus, our study population encompasses the age range over which accommodative decline is most pronounced. Prior morphometric histologic studies of rhesus monkey ciliary muscle have included monkeys as old as 29 and 34 years.1,9

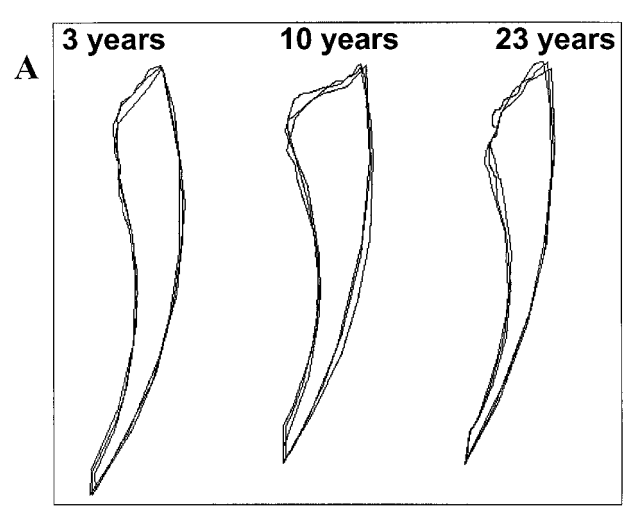
Both iridectomized and non-iridectomized monkey eyes were examined here. The absence of the iris is unlikely to influence the homatropinized configuration of the ciliary region. Maximum accommodation induced by corneal carbachol iontophoresis is reduced in iridectomized eyes, but submaximal accommodation induced by systemic intramuscular pilocarpine infusion and maximum centrally stimulated accommodation, both of which probably better reflect more "normal physiological" accommodation, is not reduced.²¹ Therefore, iridectomy is unlikely to alter the normal physiology or accommodative mechanism.

UBM is used for clinical diagnosis of the anterior segment anomalies. 12, 22-25 Here, we describe the normal anatomy of the monkey ciliary region and to look for changes with age in the living, homatropinized monkey eye using UBM. We have previously used UBM imaging of the rhesus monkey ciliary region

^b A positive value indicates that the measurement was larger in the temporal quadrant.

^c Probability that mean = 0 by the two-tailed paired t-test.

^d CB, ciliary body; CM, ciliary muscle.



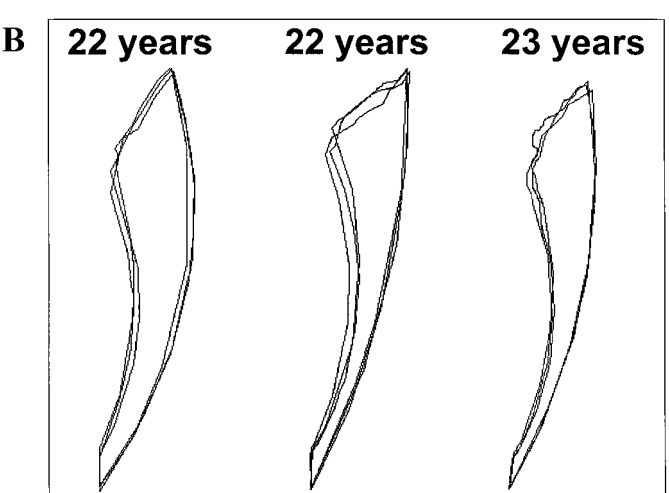
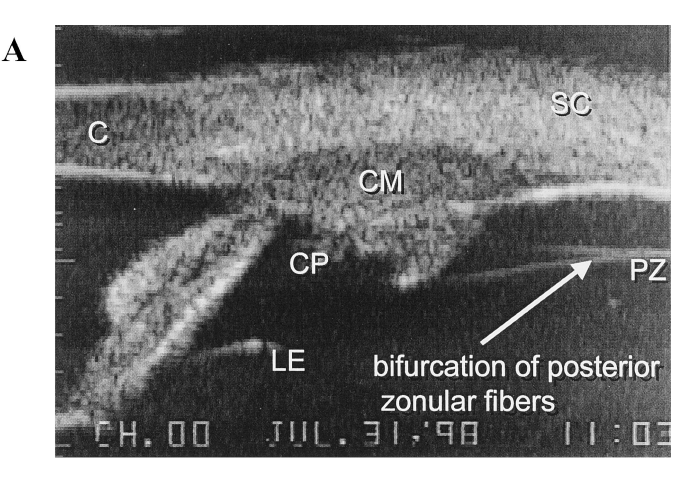


FIGURE 6.

Tracings of the nasal ciliary body region from three separate images from (A) three monkeys of widely differing ages and (B) three monkey of similar ages. Tracings suggest no age-dependent differences.

during centrally stimulated accommodation to show that the inner apex of the ciliary muscle moves forward and toward the axis of the eye and, in accordance with histologic findings,² that the posterior zonular fiber length is extended during accommodation.²⁶

UBM has also been used previously to observe normal¹⁰ and abnormal arrangement of the human anterior zonule.²⁷ The resolution of a 50-MHz UBM is sufficient to visualize the zonular fiber bundles. The 50-MHz transducer provides ~50-µm lateral resolution and ~40-µm axial resolution (depth), 10 and the zonular fiber bundles of human eyes are 20 to 80 µm in diameter. 28 Although some individual zonular fibers may be smaller than the resolution of the UBM, the larger fibers and the zonular fiber bundles can clearly be resolved. 10, 27 With minimal manipulation of the eye and the UBM transducer, the course of the posterior zonular fibers can be followed. The appearance of the bifurcations and similarities with prior SEM studies indicates that these structures are zonular fibers and not vitreous face. Furthermore, when the UBM transducer oscillation is in the plane parallel to the fibers, they appear continuous, whereas when the oscillation is orthogonal, they appear as multiple cross sections through a meshwork, confirming that they are indeed composed of multiple fiber bundles.



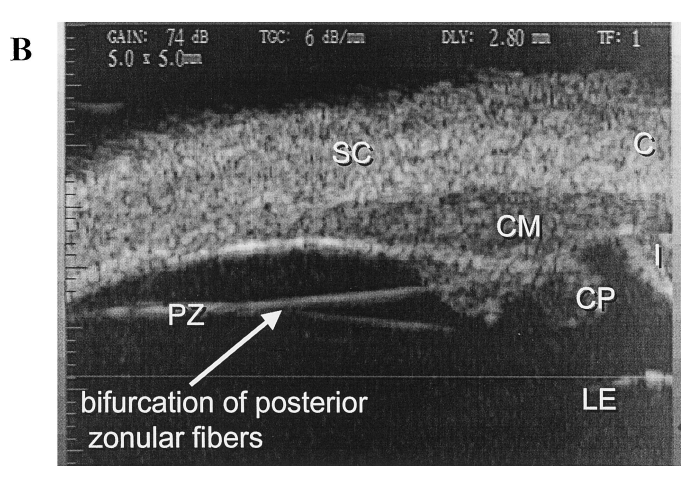


FIGURE 7.

Bifurcation of the posterior zonular fibers was observed frequently from the UBM images, most commonly in the temporal quadrant of the eye as shown here in two different monkeys. Zonular bifurcation was observed less frequently and less distinctly in the nasal quadrant of the eye, perhaps due to an inability to image the nasal zonular fibers as clearly as the temporal fibers. C, cornea; CM, ciliary muscle; CP, ciliary process; I, iris; PZ, posterior zonule; SC, sclera; LE, lens equator.

The anterior and posterior zonular fibers are not generally visible simultaneously because of their different orientations, but when both groups lie orthogonal to the orientation of the incident ultrasound beam, both can be seen (Fig. 8).

The ciliary region measured from UBM images (the region between the inner surface of the sclera and the inner surface of the ciliary body) includes the ciliary muscle and perhaps the ciliary body ground plate and stroma. The same criteria have been used for all animals and for both the nasal and temporal quadrants. Thus, although the nasal/temporal differences cannot be attributed specifically to the ciliary muscle, they do reflect differences in morphometry of the ciliary region, most of which comprises the muscle. It is possible that age-dependent differences within the ciliary muscle, as identified from histologic studies, were not observed here because UBM is unable to sharply differentiate the muscle from contiguous structures in the ciliary region.

The outline of the ciliary region from which measurements were made was readily identifiable in each image. Static images were grabbed off of real-time video tape and although the landmarks used for tracing the overlays are not always distinct in the static

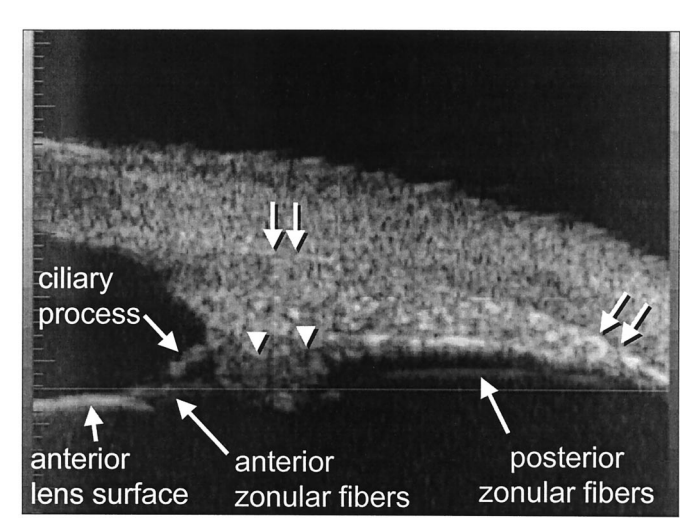


FIGURE 8.

UBM image showing both the anterior and posterior zonular fibers in the nasal ciliary region of an appropriately oriented eye. The anterior zonular fibers extend between the anterior lens surface and the tips of the ciliary processes. One of the ciliary processes appears as a protrusion from the ciliary body. The paired arrows show the demarcation between the ciliary muscle and the sclera. Paired arrowheads identify the demarcation between the ciliary muscle and the stroma of the ciliary body.

images (e.g., the scleral spur in Fig. 2B is very close to the edge of the UBM image), these landmarks were distinct on the real-time video. The real-time video aided in the identification of the posterior zonular fibers, the boundary between the sclera and the ciliary body, the scleral spur, and the inner edge of the ciliary body. The anterior edge of the ciliary body is also reasonably clear, especially in the absence of the iris. Subjective identification of this boundary may have resulted in increased variability of our measurements (ciliary body area for example), but is unlikely to influence any of the conclusions drawn. Clear differentiation can be made between the anterior edge of the ciliary body and the protruding ciliary processes (Fig. 3 A and B).

UBM provides reliable and reproducible images for comparison of similar views of the ciliary body in different monkeys. The real-time video display allows the probe position to be manipulated and reoriented to obtain the precise view required. The limited image resolution and lack of distinction between different tissue types reduces the accuracy of a morphometric analysis compared with histology. The limited sampling of selected UBM images from which measurements were taken and the subjective nature of the outlining of the ciliary region may result in bias. Nonetheless, the naso-temporal zonular asymmetries and the substantially larger zonular-ciliary body space on the temporal quadrant have not been observed previously by light microscopy or SEM, perhaps because of artifactual changes that may be introduced by the relatively harsh treatment required for fixation, processing, and microscopy. Our UBM observation of nasal/temporal asymmetry is in accordance with increased temporal ciliary body length in the human^{29, 30} and nasal/temporal asymmetries previously identified histologically in the avian eye.^{31, 32} The asymmetry is not a consequence of asymmetric stretching of the globe to orient the eye for UBM imaging because (1) the globe is not stretched, (2) the same technique and tension is used to image both the nasal and temporal sides, (3) in humans, the degree of adduction and abduction required to achieve this eye position can readily be achieved voluntarily, and (4) the same zonular arrangements and nasal/temporal asymmetries have been observed with UBM in enucleated human eyes (Glasser, unpublished observations). As has been suggested for other animal species, 31 ocular asymmetries may represent the functional anatomy required to orient the optical axis of the crystalline lens toward the point of regard during convergence and accommodation in primates.

A role in the pathophysiology of presbyopia is not immediately apparent from our findings of a tendency for increasing outer ciliary muscle radius in the nasal quadrant and decreased inner ciliary muscle radius in the temporal quadrant with increasing age. Although previous histologic study of the rhesus monkey ciliary muscle identified age-dependent morphometric changes with possible implications for the development of presbyopia, 1, 2, 4 the present study, using objective geometric morphologic criteria on digital UBM images, did not. Especially elusive in these images is the posterior termination of the ciliary muscle. For the purposes of this study, this point was designated, rightly or wrongly, but consistently and objectively, as the posterior point of attachment of the posterior zonular fibers to the ciliary body.

We have found a significant decrease in temporal circumlental space with age in the monkey eye, a characteristic of the aging human eye that has been documented previously in vitro with SEM³³ and in vivo with MRI.¹⁷ This is unlikely to be due to a supposed growth-related increase in equatorial diameter of the lens^{34, 35} because in vivo MRI measurements of unaccommodated eyes show no age-dependent increase in lens equatorial diameter. 17 The suggested age-related increase in lens diameter³⁵ stems from a study by Smith³⁶ on isolated lenses. However, Smith recognized that when isolated, the lens tends to become accommodated, relatively more so for young lenses than for old.³⁶ Hence, the agedependent increase in diameter of isolated lenses more likely reflects accommodation-related rather than growth-related changes. In humans, the decrease in circumlental space may be due to configurational changes in the ciliary muscle. However, this has not been documented to occur in the aging rhesus monkey ciliary muscle, and our UBM images (Fig. 6) show no evidence of it. No in vivo or in vitro measurements of monkey lens diameters are available to resolve the etiology of the decrease in circumlental space in monkey eyes. The theory attributing presbyopia in humans to increasing lens equatorial diameter³⁴ seems fundamentally flawed because both of its underpinning principles—increased lens equatorial diameter and outward movement of the lens equator during accommodation—seem invalid. Furthermore, the generalized zonular arrangement observed here confirms the anatomical descriptions from SEM,²⁰ but shows no insertion of zonular fibers onto the anterior face of the ciliary muscle as has been postulated to play an essential role in this novel accommodative mechanism^{34, 37}

We have identified posterior zonules coursing through the vitreous, separated from the pars plana ciliary body, contravening Rohen's²⁰ scanning electron microscopic studies. This is in all likelihood due to the artifact of the posterior zonules lying against the pars plana in the fixed, sectioned eye in the SEM studies in which the natural zonular fiber tension and position has been disrupted.

ACKNOWLEDGMENTS

This work was funded by grants from the National Eye Institute, National Institutes of Health EY10213 (PLK) and EY07119 (David L. DeMets, PhD); RR00167 to the Wisconsin Regional Primate Research Center; Research to Prevent Blindness; and Johnson & Johnson. LB was supported by National Eye Institute, National Institutes of Health grant EY07119.

Received October 11, 2000; revision received January 22, 2001.

REFERENCES

- Tamm S, Tamm E, Rohen JW. Age-related changes of the human ciliary muscle: a quantitative morphometric study. Mech Ageing Dev 1992;62:209–21.
- Lutjen-Drecoll E, Tamm E, Kaufman PL. Age-related loss of morphologic responses to pilocarpine in rhesus monkey ciliary muscle. Arch Ophthalmol 1988;106:1591–8.
- Bito LZ, DeRousseau CJ, Kaufman PL, Bito JW. Age-dependent loss of accommodative amplitude in rhesus monkeys: an animal model for presbyopia. Invest Ophthalmol Vis Sci 1982;23:23–31.
- Lutjen-Drecoll E, Tamm E, Kaufman PL. Age changes in rhesus monkey ciliary muscle: light and electron microscopy. Exp Eye Res 1988;47:885–99.
- Poyer JF, Kaufman PL, Flugel C. Age does not affect contractile responses of the isolated rhesus monkey ciliary muscle to muscarinic agonists. Curr Eye Res 1993;12:413–22.
- Gabelt BT, Kaufman PL, Polansky JR. Ciliary muscle muscarinic binding sites, choline acetyltransferase, and acetylcholinesterase in aging rhesus monkeys. Invest Ophthalmol Vis Sci 1990;31:2431–6.
- 7. Glasser A, Campbell MC. Presbyopia and the optical changes in the human crystalline lens with age. Vision Res 1998;38:209–29.
- Glasser A, Campbell MC. Biometric, optical and physical changes in the isolated human crystalline lens with age in relation to presbyopia. Vision Res 1999;39:1991–2015.
- 9. Tamm E, Lutjen-Drecoll E, Jungkunz W, Rohen JW. Posterior attachment of ciliary muscle in young, accommodating old, presbyopic monkeys. Invest Ophthalmol Vis Sci 1991;32:1678–92.
- 10. Pavlin CJ, Foster FS. Ultrasound Biomicroscopy of the Eye. New York: Springer-Verlag, 1995:3–16.
- 11. Bacskulin A, Gast R, Bergmann U, Guthoff R. Ultrasound biomicroscopy imaging of accommodative configuration changes in the presbyopic ciliary body. Ophthalmologe 1996;93:199–203.
- 12. Marchini G, Pagliarusco A, Toscano A, Tosi R, Brunelli C, Bonomi L. Ultrasound biomicroscopic and conventional ultrasonographic study of ocular dimensions in primary angle-closure glaucoma. Ophthalmology 1998;105:2091–8.
- 13. Trindade F, Pereira F, Cronemberger S. Ultrasound biomicroscopic imaging of posterior chamber phakic intraocular lens. J Refract Surg 1998;14:497–503.
- 14. Kobayashi H, Kobayashi K. Quantitative comparison of Zeiss-Humphrey model 840 and Rion UX-02 systems of ultrasound biomicroscopy. Graefes Arch Clin Exp Ophthalmol 1999;237:381–6.
- Castanheira VRC, Zanoto A, Malta RFS, Betinjanea J. Ultrasound biomicroscopic (UBM) quantitative analysis of ocular changes during accommodation. Invest Ophthalmol Vis Sci 2000;41:S564.
- Semmlow JL, Strenk SA, Strenk LM, Munoz P, Epstein D, DeMarco JK. High resolution MRI of the accommodated lens and ciliary muscle. In: Vision Science and its Applications. OSA Technical Digest Series. Washington, DC: Optical Society of America, 1999:118–21.
- Strenk SA, Semmlow JL, Strenk LM, Munoz P, Gronlund-Jacob J, DeMarco JK. Age-related changes in human ciliary muscle and lens: a magnetic resonance imaging study. Invest Ophthalmol Vis Sci 1999;40:1162–9.

- 18. Glasser A, Croft M, Kaufman PL. A morphometric ultrasound biomicroscopic study of the aging rhesus monkey ciliary region In: Vision Science and its Applications. OSA Technical Digest Series. Washington, DC: Optical Society of America, 1999:126–9.
- 19. Farnsworth PN, Burke P. Three-dimensional architecture of the suspensory apparatus of the lens of the Rhesus monkey. Exp Eye Res 1977;25:563–76.
- Rohen JW. Scanning electron microscopic studies of the zonular apparatus in human and monkey eyes. Invest Ophthalmol Vis Sci 1979;18:133–44.
- Crawford KS, Kaufman PL, Bito LZ. The role of the iris in accommodation of rhesus monkeys. Invest Ophthalmol Vis Sci 1990;31: 2185–90.
- 22. Azuara-Blanco A, Spaeth GL, Araujo SV, Augsburger JJ, Katz LJ, Calhoun JH, Wilson RP. Ultrasound biomicroscopy in infantile glaucoma. Ophthalmology 1997;104:1116–9.
- 23. Yuki T, Kimura Y, Nanbu S, Kishi S, Shimizu K. Ciliary body and choroidal detachment after laser photocoagulation for diabetic retinopathy: a high-frequency ultrasound study. Ophthalmology 1997;104:1259–64.
- 24. Marigo FA, Finger PT, McCormick SA, Iezzi R, Esaki K, Ishikawa H, Seedor J, Liebmann JM, Ritch R. Anterior segment implantation cysts: ultrasound biomicroscopy with histopathologic correlation. Arch Ophthalmol 1998;116:1569–75.
- 25. Deramo VA, Shah GK, Baumal CR, Fineman MS, Correa ZM, Benson WE, Rapuano CJ, Cohen EJ, Augsburger JJ. Ultrasound biomicroscopy as a tool for detecting and localizing occult foreign bodies after ocular trauma. Ophthalmology 1999;106:301–5.
- Glasser A, Kaufman PL. The mechanism of accommodation in primates. Ophthalmology 1999;106:863–72.
- 27. Pavlin CJ, Buys YM, Pathmanathan T. Imaging zonular abnormalities using ultrasound biomicroscopy. Arch Ophthalmol 1998;116:854–7.
- Kaczurowski, MI. Zonular fibers of the human eye. Am J Ophthalmol 1964;58:1030–47.
- 29. Hogan MJ, Alvarado JA, Weddell JE. Histology of the Human Eye: an Atlas and Textbook. Philadelphia: Saunders, 1971.
- Strenk SA, Strenk LM, Semmlow JL. High resolution MRI study of circumlental space in the aging eye. J Refract Surg 2000;16:S659–60.
- 31. Glasser A, Troilo D, Howland HC. The mechanism of corneal accommodation in chicks. Vision Res 1994;34:1549–66.
- 32. Murphy CJ, Glasser A, Howland HC. The anatomy of the ciliary region of the chicken eye. Invest Ophthalmol Vis Sci 1995;36: 889–96.
- 33. Farnsworth PN, Shyne SE. Anterior zonular shifts with age. Exp Eye Res 1979;28:291–7.
- Schachar RA, Black TD, Kash RL, Cudmore DP, Schanzlin DJ. The mechanism of accommodation and presbyopia in the primate. Ann Ophthalmol 1995;27:58–67.
- 35. Rafferty NS. Lens morphology. In: Maisel H, ed. The Ocular Lens Structure, Function, and Pathology. New York: Marcel Dekker, 1985:1–60.
- 36. Smith P. Diseases of the crystalline lens and capsule: on the growth of the crystalline lens. Trans Ophthalmol Soc UK 1883;3:79–102.
- 37. Schachar RA, Anderson D. The mechanism of ciliary muscle function. Ann Ophthalmol 1995;27:126–32.

Adrian Glasser

College of Optometry 4901 Calhoun Road University of Houston Houston, Texas 77004 e-mail: AGlasser@popmail.opt.uh.edu